

($d, {}^3\text{He}$) Reactions on the Even Zirconium Isotopes*†

B. M. FREEDOM† AND E. NEWMAN
Oak Ridge National Laboratory, Oak Ridge, Tennessee

AND

J. C. HIEBERT§
Texas A & M University, College Station, Texas

(Received 13 October 1967)

An investigation of the proton ground-state configurations in the even zirconium isotopes ($A=90, 92, 94, 96$) was undertaken using the ($d, {}^3\text{He}$) reaction at a deuteron energy of 34.4 MeV. The experimental angular distributions were compared with distorted-wave calculations in the finite-range approximation which include nonlocality in the distorted waves. The residual yttrium isotopes ($A=89, 91, 93, 95$) have $\frac{1}{2}^-$ ground states, and the observed spectra can be interpreted in terms of a simple shell-model picture which considers hole and particle configurations in the $1g_{9/2}$, $2p_{1/2}$, $2p_{3/2}$, and $1f_{5/2}$ proton shells and allowed couplings in the $2d_{5/2}$ neutron shell. It was found that the filling of the $2d_{5/2}$ neutron shell apparently has a measurable effect on the relative amounts of the $(2p_{1/2})^2$ and $(1g_{9/2})^2$ proton admixtures in the zirconium ground states. The strength of the $(2p_{1/2})^2$ term in the ground-state wave functions was determined to be: 64% for ${}^{90}\text{Zr}$, 55% for ${}^{92}\text{Zr}$, 66% for ${}^{94}\text{Zr}$, and 86% for ${}^{96}\text{Zr}$.

I. INTRODUCTION

IN the mass region $A=90$, the shell model has been comparatively successful in accounting for the observed level structure.^{1,2} The shell-model calculations make assumptions about the effective proton-neutron interaction in this region and thus provide impetus for experimental measurements to test the validity of such assumptions. One such test can be furnished by a quantitative study of the proton configurations in this region. Pickup reactions are a sensitive tool for investigating target ground-state wave functions and, in most cases, will reveal admixtures of single-particle configurations. Recent examples of the proton pickup reaction are the (n, d) ,³ ($d, {}^3\text{He}$),⁴⁻⁷ and (t, α) ⁸ experiments.

Previous ($d, {}^3\text{He}$) reaction studies on nuclei in this mass region have used deuterons with energies on the

order of 20 MeV.^{6,7} Because of the negative Q value of this reaction and the relatively high Coulomb barrier for the exit channel, these previous investigations were limited in the number of nuclei that could be studied and in the range of excitation observed. These problems are less restrictive with the increased deuteron energy (34.4 MeV) used in this work. In addition, the higher incident energy results in highly structured angular distributions with decidedly different shapes for each angular momentum (l) transferred.

A simple shell-model interpretation of the ${}^{90}\text{Zr}$ nucleus predicts a minor closure at the $2p_{1/2}$ proton shell ($Z=40$) and a major closure at the $1g_{9/2}$ neutron shell ($N=50$). For the zirconium isotopes with $A>90$, one may expect the additional neutrons to enter the $2d_{5/2}$ shell which fills at ${}^{96}\text{Zr}$. It is well known,^{2,6-12} however, that the ${}^{90}\text{Zr}$ ground state is an admixture of the $(2p_{1/2})^2$ and $(1g_{9/2})^2$ proton configurations. Thus, the zirconium isotopes are particularly suited to study the effect on a mixed proton configuration caused by filling a neutron shell.

The experimental angular distributions obtained in the present study leading to states in the yttrium isotopes are analyzed using the distorted-wave (DW) theory. The sensitivity of the analysis to various parts of the calculations is also investigated.

II. EXPERIMENTAL PROCEDURE

With the 34.4-MeV deuteron beam from the Oak Ridge isochronous cyclotron, differential cross sections were measured for ($d, {}^3\text{He}$) reactions on the stable even isotopes of zirconium. The energy of the beam was

* Research sponsored by the U. S. Atomic Energy Commission under contract with Union Carbide Corporation.

† Results of this work were submitted by one of us (BMP) in partial fulfillment of the requirements for a Ph.D. degree, University of Tennessee.

‡ Oak Ridge Graduate Fellow from the University of Tennessee under appointment from Oak Ridge Associated Universities; present address: Cyclotron Laboratory, Michigan State University, East Lansing, Mich.

§ Visiting scientist at Oak Ridge National Laboratory, 1965-1966.

¹ K. H. Bhatt and J. B. Ball, Nucl. Phys. **63**, 286 (1965); N. Auerbach and I. Talmi, *ibid.* **64**, 458 (1965).

² J. Vervier, Nucl. Phys. **75**, 17 (1966).

³ I. Ilakovic, L. G. Kuo, M. Petracic, I. Slaus, P. Tomas, and G. R. Satchler, Phys. Rev. **128**, 2739 (1962); W. N. Wang and E. J. Winhold, *ibid.* **140**, B882 (1965); G. Chursin, M. Fazio, S. Micheletti, M. Pignaneli, and L. Zetta, Nucl. Phys. **A93**, 209 (1967).

⁴ J. C. Hiebert, E. Newman, and R. H. Bassel, Phys. Rev. **154**, 898 (1967).

⁵ J. L. Yntema and G. R. Satchler, Phys. Rev. **134**, B976 (1964); B. Cujec, *ibid.* **128**, 2303 (1962).

⁶ J. L. Yntema, Phys. Letters **11**, 140 (1964).

⁷ C. D. Kavaloski, J. S. Lilley, D. C. Shreve, and Nelson Stein, University of Washington Nuclear Physics Laboratory Annual Report, 1966, p. 22 (unpublished); Phys. Rev. **161**, 1107 (1967).

⁸ D. D. Armstrong and A. G. Blair, Bull. Am. Phys. Soc. **11**, 752 (1966).

⁹ B. F. Bayman, A. S. Reiner, and R. K. Sheline, Phys. Rev. **115**, 1627 (1959).

¹⁰ S. Cohen, R. D. Lawson, M. H. MacFarlane, and M. Soga, Phys. Letters **10**, 195 (1964).

¹¹ R. B. Day, A. G. Blair, and D. D. Armstrong, Phys. Letters **9**, 327 (1964).

¹² C. B. Fulmer and J. B. Ball, Phys. Rev. **140**, B330 (1965).

determined to within ± 0.1 MeV from the magnetic field of a 153° analyzing magnet. The targets, in the form of thin, self-supporting foils, were obtained from the ORNL Isotopes Division. The thicknesses were determined by weighing. These values were checked by using α -particle ranges with an ${}^{241}\text{Am}$ source and by small-angle Rutherford (${}^3\text{He}, {}^3\text{He}$) elastic scattering at 30.7 MeV. The thicknesses remain, however, the largest uncertainty in the absolute values of the cross sections. The errors associated with them have been taken to be 10%.

The reaction products were detected in a ΔE - E detector telescope for particle identification. The telescope consisted of silicon surface-barrier counters with thicknesses of $200\ \mu$ for ΔE and $500\ \mu$ for E . This combination of detectors allowed the observation of ${}^3\text{He}$ particles with energies between 16.5 and 34 MeV.

The E and ΔE pulses were added at the amplifier input and ΔE versus $(E + \Delta E)$ spectra were recorded in a 20 000-channel, multiparameter pulse-height analyzer. Figure 1 shows the ${}^3\text{He}$ spectra observed from $(d, {}^3\text{He})$ reactions on ${}^{90}\text{Zr}$, ${}^{94}\text{Zr}$, and ${}^{96}\text{Zr}$ at a lab angle of 20.0° and on ${}^{92}\text{Zr}$ at 20.5° . The resolution (full width at half-maximum, FWHM) ranges from 75 keV for ${}^{90}\text{Zr}$ to 125 keV for ${}^{92}\text{Zr}$. This difference in resolution is mainly due to the target thickness. The energy scale for each of the spectra is approximately the same and the position of the ${}^{89}\text{Y}$ ground state has been aligned vertically. The dominant peaks are labeled at the top of each spectrum with Roman numerals that correspond to those identifying the angular distributions in subsequent figures.

Making the appropriate relativistic kinematic corrections, the energy scale for each spectrum was calibrated from the Q values¹³ for the $(d, {}^3\text{He})$ ground-state reactions on ${}^{90}\text{Zr}$ (-2.89 MeV), ${}^{92}\text{Zr}$ (-3.90 MeV), ${}^{94}\text{Zr}$ (-4.81 MeV), and the ${}^{16}\text{O}$ impurity (-6.63 MeV).

TABLE I. Variation of calculated differential cross sections with the parameters of the bound-state potential.^a

(n, l, j)	r_0 (F)	$\lambda = 20$		$\lambda = 25$	
		$a = 0.65$ F	$a = 0.70$ F	$a = 0.65$ F	$a = 0.70$ F
$2p_{1/2}$	1.200	1.03	1.18	1.0	1.14
	1.225	1.24	1.40	1.20	1.36
	1.250	1.47	1.67	1.43	1.62
$2p_{3/2}$	1.200	0.99	1.11	1.0	1.12
	1.225	1.17	1.31	1.18	1.32
	1.250	1.37	1.54	1.39	1.56
$1f_{5/2}$	1.200	1.08	1.22	1.0	1.14
	1.225	1.33	1.49	1.23	1.39
	1.250	1.63	1.80	1.52	1.71
$1g_{9/2}$	1.200	0.94	1.06	1.0	1.12
	1.225	1.17	1.31	1.24	1.39
	1.250	1.46	1.63	1.54	1.72

^a The values are in ratio to the predictions with: $r_0 = 1.20$ F, $a = 0.65$ F, and $\lambda = 25$.

¹³ J. H. E. Mattauch, W. Thiele, and A. H. Wapstra, Nucl. Phys. **67**, 1 (1965).

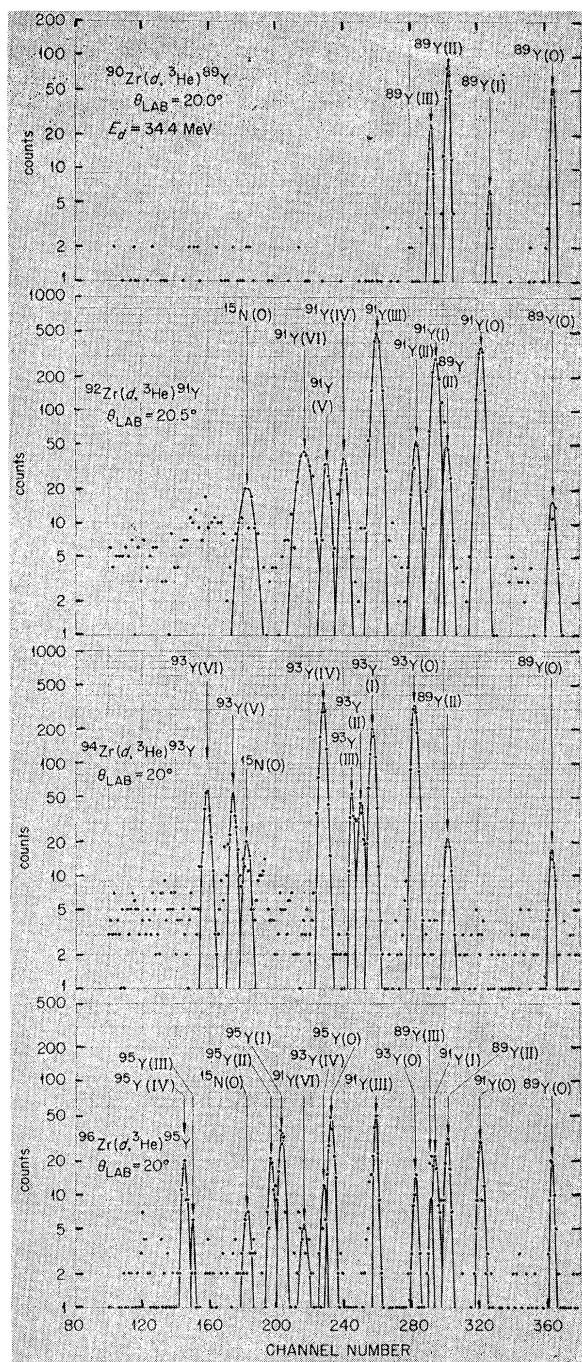


FIG. 1. Experimental spectra of ${}^3\text{He}$ particles resulting from $(d, {}^3\text{He})$ reactions on ${}^{90}\text{Zr}$, ${}^{92}\text{Zr}$, ${}^{94}\text{Zr}$, and ${}^{96}\text{Zr}$.

The excitation energies for all states and the mass of ${}^{95}\text{Y}$ were determined from a broad-range magnetic spectrograph spectrum from the ${}^{96}\text{Zr}$ target at 20° (L). The ${}^{96}\text{Zr}$ target was enriched to only 57% with substantial amounts of each of the other Zr isotopes. Thus the spectra taken with this target provided a cross check for the energy assignments. The uncertainties in the

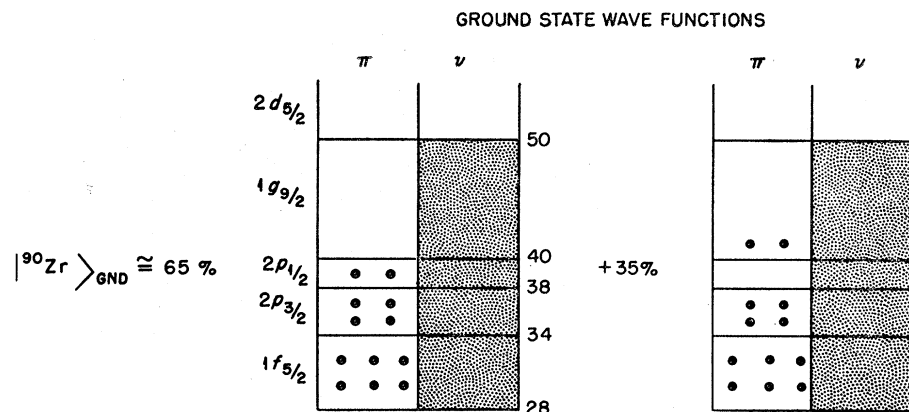


FIG. 2. Shell-model picture of the ^{90}Zr ground state.

excitation energies of the residual yttrium isotopes are ± 20 keV.

Relative errors for each cross-section measurement are indicated in the experimental angular distributions. Where no error bar is shown, the relative error is less than the size of the data point. The uncertainties in the absolute cross sections are due mainly to the error in the values of the target thicknesses. As was stated above, these values are not known to better than 10%. All other systematic errors can be folded into this uncertainty, yielding an error which is on the order of 15%.

III. THEORETICAL INTERPRETATION

A. Distorted-Wave Analysis

The application of the distorted-wave theory to ($d, {}^3\text{He}$) reactions has been studied in detail by Hiebert, Newman, and Bassel.⁴ They investigated the effects of both finite-range and nonlocality in the ($d, {}^3\text{He}$) reaction and found that the best results were obtained using finite-range and nonlocal corrections together. The distorted-wave (DW) calculations⁴ presented here for comparison with experimental angular distributions make use of their conclusions. Two types of distorted-wave calculations are presented in this work: The first is the usual local zero-range (LZR) calculation and the second is the calculation (FRNL) in the local-energy approximation which includes corrections both for finite-range and, in the optical-model potentials, for nonlocality.

Also in Ref. 4, spin-orbit effects, radial cutoffs, and approximations to the bound-state well were investigated. It was concluded that (1) spin-orbit interactions should be included; (2) radial cutoffs in the integrations need not be used; and (3) the bound-state function for good single-particle states, assuming the orbital to be an eigenfunction of a Woods-Saxon well, is best repre-

sented with the energy eigenvalue equal to the observed separation energy.

Since the parameters of the bound-state well have not been uniquely determined by experiment,^{15,16} an investigation of their effect on the DW calculations was made for variations within a realistic range of values. It was found that the magnitude, but not the shape, of the angular distributions is quite sensitive to small changes in the radius parameter r_0 , the diffusivity a , and to a lesser degree in the spin-orbit strength λ . This sensitivity is displayed in Table I. The proton binding energy, and thus the Q value, was the same for all of the calculations in order to exclude any Q dependence. However, the well depth was allowed to vary so that each set of parameters would have the binding energy as an eigenvalue. From the table it is seen that small variations in r_0 and a can lead to quite large variations in the calculated strengths. This effect arises because the DW contributions to the ($d, {}^3\text{He}$) reaction occur at the nuclear surface. In terms of the bound-state function, an increase in the values of r_0 and/or a results in a shallower well in order to keep the binding-energy constant, thereby increasing the tail of the wave function and, correspondingly, the overlap with the distorted waves at the surface. In this way, the calculated cross section is enhanced. As may be inferred from the table, a change in the spin-orbit strength λ from 20 to 25 produces a change in the cross section that is proportional to l for $j=l+\frac{1}{2}$ and to $-(l+1)$ for $j=l-\frac{1}{2}$. This result is expected from perturbation theory. The sensitivity of the cross section to a change in this spin-orbit strength is much weaker than is the case of a variation in r_0 and/or a . Similar calculations varying the bound-state parameters were made for different Q values. It was found that the trends in the variations of the predicted strengths, characterized by Table I, were only slightly Q -dependent.

One set of bound-state parameters was chosen from physical considerations and was used for all of the DW calculations that are compared with the experimental

¹⁴ The IBM-7090 code JULIE was used for all DW calculations. R. H. Bassel, R. M. Drisko, and G. R. Satchler, Oak Ridge National Laboratory Report No. ORNL-3240 (unpublished); and Oak Ridge National Laboratory Memorandum to the Users of the Code JULIE, 1966 (unpublished).

¹⁵ R. H. Bassel, Phys. Rev. 149, 791 (1966).

¹⁶ R. M. Drisko and R. H. Bassel (private communication).

TABLE II. Optical-model parameters.

Reaction	Target	V (MeV)	r_0 (F)	a (F)	W (MeV)	W_D (MeV)	r_0' (F)	a' (F)	V_{s0} (MeV)
$(d,d)^a$	${}^{90}\text{Zr}$	97.99	1.098	0.806	...	12.26	1.310	0.813	6.75
	${}^{92}\text{Zr}$	97.92	1.099	0.818	...	12.78	1.280	0.827	6.17
	${}^{94}\text{Zr}$	97.74	1.091	0.834	...	15.28	1.250	0.815	7.00
	${}^{96}\text{Zr}$	97.92	1.088	0.840	...	15.19	1.245	0.820	7.50
$({}^3\text{He}, {}^3\text{He})^b$	${}^{89}\text{Y}$	172.0	1.140	0.723	17.00	...	1.550	0.800	...
	${}^{89}\text{Y}$	154.4	1.227	0.668	18.72	...	1.510	0.800	...

^a $r_c = 1.3$ F.^b $r_c = 1.4$ F.

distributions in the following sections. The values for r_0 and a were determined from an optical-model potential that describes proton scattering from ${}^{40}\text{Ar}$ and ${}^{42}\text{Ca}$.¹⁷ They also give a good account of the ${}^{16}\text{O}(d, {}^3\text{He}){}^{15}\text{N}$ and ${}^{40}\text{Ca}(d, {}^3\text{He}){}^{39}\text{K}$ reactions.⁴ These parameters are $r_0 = 1.2$ F, $a = 0.65$ F, $r_c = 1.25$ F, and $\lambda = 25$. The choice of $\lambda = 25$ is appropriate to the spin-orbit strength in both the shell model and the optical potential.¹⁸

The general form of the DW theory includes spin-orbit effects in both the distorted waves and the bound-state function. This complete calculation was made for the $l=1$ transfers; but for $l=3$ and $l=4$ transfers, because of computer memory limitations, a spin-orbit interaction could be included only in the bound-state well. Although these latter calculations cannot be expected to reproduce any shape dependence on the total angular momentum j transferred,¹⁹ they are expected to be otherwise reliable.

The optical-model parameters used in the DW calculations are listed in Table II. The deuteron parameters are the values that gave the best fit to elastic scattering at 34.4 MeV from the zirconium isotopes.²⁰ Distorted-wave calculations using an average set of parameters obtained in that investigation were essentially equivalent in shape and magnitude to the DW calculations using the best fit values. The ${}^3\text{He}$ parameters were obtained from a study of ${}^3\text{He}$ elastic scattering from ${}^{89}\text{Y}$ at 24.7, 30.7, and 41.0 MeV.²¹ The set with $V = 172$ MeV adequately reproduced the observed scattering at the three energies. The parameters with $V = 154.4$ MeV fit the observed scattering at 30.7 MeV equally well and their use in the DW calculations will be discussed in Sec. IV A.

B. Shell Model

Considering the ${}^{90}\text{Zr}$ nucleus as having two protons outside of a ${}^{88}\text{Sr}$ core, previous investigators^{2,6-12} have

¹⁷ L. L. Lee, Jr., J. P. Schiffer, B. Zeidman, G. R. Satchler, R. M. Drisko, and R. H. Bassel, Phys. Rev. **136**, B971 (1964).

¹⁸ R. H. Bassel (private communication).

¹⁹ B. M. Freedom, E. Newman, and J. C. Hiebert, Phys. Letters **22**, 657 (1966).

²⁰ E. Newman, L. C. Becker, B. M. Freedom, and J. C. Hiebert, Nucl. Phys. **A100**, 225 (1967).

²¹ M. R. Cates, B. M. Freedom, E. Newman, and J. C. Hiebert (unpublished).

described the ground state in terms of a configuration mixture of approximately 65% $(2p_{1/2})^2$ plus 35% $(1g_{9/2})^2$. A shell-model picture of this mixture is shown in Fig. 2. The wave function corresponding to this picture may be written as

$$|{}^{90}\text{Zr}\rangle_{\text{Gnd}} = [A_{90}|\pi(2p_{1/2})^2\rangle + B_{90}|\pi(1g_{9/2})^2_0\rangle] |{}^{88}\text{Sr}\rangle.$$

Assuming that the additional neutrons in the ground states of the other even zirconium isotopes populate only the $2d_{5/2}$ shell, then the two $1g_{9/2}$ protons in ${}^{92}\text{Zr}$ can couple with the allowed 0^+ , 2^+ , and 4^+ couplings

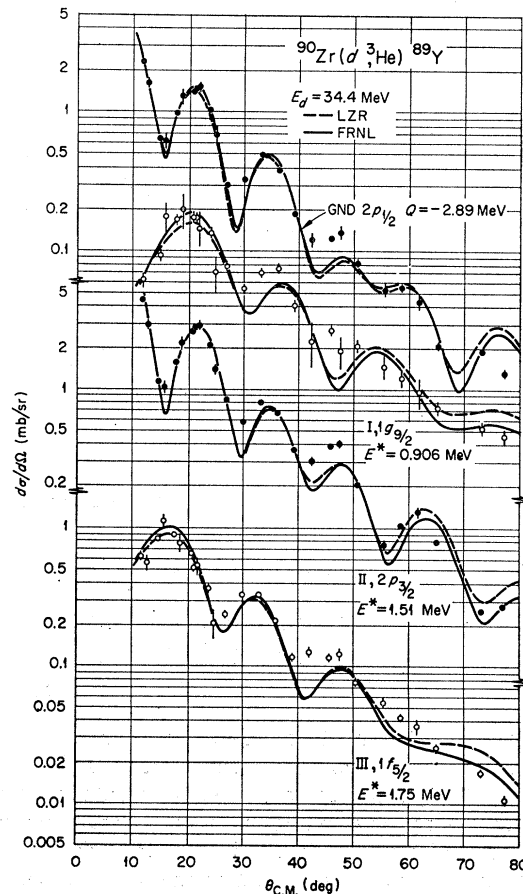
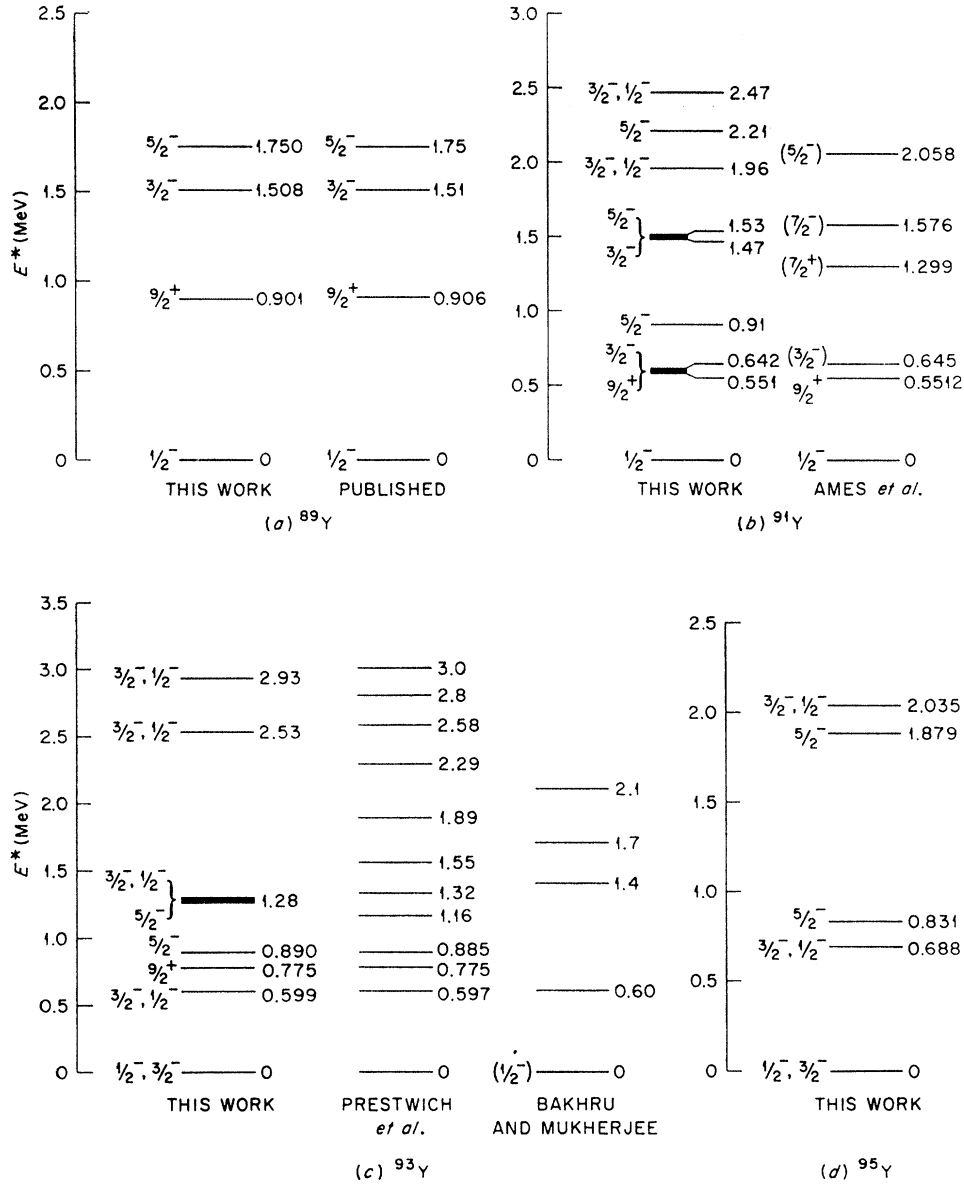


FIG. 3. Angular distributions for ${}^{90}\text{Zr}(d, {}^3\text{He}){}^{89}\text{Y}$ with LZR and FRNL distorted-wave calculations.

FIG. 4. Energy levels of ^{89}Y , ^{91}Y , ^{93}Y , and ^{95}Y .

of the neutrons to give the wave function

$$|^{92}\text{Zr}\rangle_{\text{Gnd}} = \{A_{92}[\pi(2p_{1/2})^2]|\nu(2d_{5/2})^2\rangle_{0^+} + B_{92}'[\pi(1g_{9/2})^2]_{0^+} \times |\nu(2d_{5/2})^2\rangle_{0^+} + B_{92}''[\pi(1g_{9/2})^2]_{2^+} + |\nu(2d_{5/2})^2\rangle_{2^+}]_{0^+} + B_{92}'''[\pi(1g_{9/2})^2]_{4^+} + |\nu(2d_{5/2})^2\rangle_{4^+}]_{0^+}\} |^{88}\text{Sr}\rangle.$$

Using two $2d_{5/2}$ neutron holes, one can obtain an expression for the ^{94}Zr ground state that is similar to that of ^{92}Zr . And since six neutrons would close the $2d_{5/2}$ shell with the above assumption, the wave function for ^{96}Zr can be written in a form similar to that of ^{90}Zr .

Extending the above model to the yttrium isotopes with one less proton, one predicts one $1/2^-$ and one $3/2^+$ state and possibly two $3/2^-$ and two $5/2^-$ hole states for

^{89}Y and ^{95}Y . The added terms in the wave functions for ^{92}Zr and ^{94}Zr could lead to two additional $3/2^+$, $3/2^-$, and $5/2^-$ states. Analyses in the following section will make use of these predictions and experimental values for the coefficients A and B in the wave functions will be compared with calculated values in Sec. V B.

IV. EXPERIMENTAL RESULTS

A. $^{90}\text{Zr}(d,^3\text{He})^{89}\text{Y}$

The experimental angular distributions for the $^{90}\text{Zr}(d,^3\text{He})^{89}\text{Y}$ reactions leading to the ground and first three excited states of ^{89}Y are shown in Fig. 3. The curves associated with each distribution are the LZR

(dashed) and FRNL (solid) DW calculations normalized to minimize χ^2 over the entire angular region. The ground and second excited state ($E^*=1.51$ MeV) result from the pickup of a $2p_{1/2}$ and a $2p_{3/2}$ proton, respectively. The j dependence displayed by the $p_{1/2}$ and $p_{3/2}$ angular distributions between 50° and 80° has been previously reported.¹⁹ From the figure one can see that there is no essential change in the predicted j dependence for the two types of calculations (LZR and FRNL) considered. The angular distribution for the first excited state ($E^*=0.906$ MeV, $\frac{3}{2}^+$) is well fit by an $l=4$ transfer and the third excited state ($E^*=1.75$ MeV, $\frac{5}{2}^-$) is likewise well described by an $l=3$ proton pickup. The spins and parities of these four states in ${}^{89}\text{Y}$ are known and, from the quality of the fits, the DW theory seems to be quite reliable in this region. As can be seen from Fig. 1, there is no evidence for the excitation of any additional states in ${}^{89}\text{Y}$ below ~ 6 MeV with a cross section $\geq 5\%$ of the ground state. In Fig. 4(a) the energy levels observed in the present experiment are compared with published²² values for the low-lying states in ${}^{89}\text{Y}$. The agreement is well within the experimental errors.

The shapes of the experimental angular distributions for this reaction may be used to determine if there is a preference for one of the types of DW calculations, or for a specific ${}^3\text{He}$ potential. Comparing the DW curves in Fig. 3, one observes that for all cases the FRNL predictions agree with the data somewhat better than the LZR calculations. This is especially true for the $l=3$ and $l=4$ transfers where the average slope of the experimental distributions is best reproduced by the FRNL curves. These minor effects are typical of the differences in shape observed for the LZR and FRNL calculations made for each isotope. In Fig. 5, FRNL calculations using ${}^3\text{He}$ optical parameters with $V=154.4$ MeV and $r_0=1.227$ F (dashed curves) are compared with the ${}^{90}\text{Zr}(d, {}^3\text{He}){}^{89}\text{Y}$ data and with the FRNL calculations previously presented in Fig. 3 (solid curves). The ${}^3\text{He}$ parameters are listed in Table II. The dashed curves have been normalized to the solid curves at the peaks near 20° . For the $2p_{1/2}$ and $2p_{3/2}$ proton transfers, the DW predictions using the set of ${}^3\text{He}$ parameters with $V=172$ MeV, $r_0=1.14$ F describe the observed distributions for angles greater than 40° better than those using the parameters with $V=154.4$ MeV. For the $l=3$ and $l=4$ cases, the dashed curves show oscillations stronger than observed and stronger than those of the solid curves. The preference for the 172-MeV set of parameters was slightly more pronounced for LZR calculations. The evidence from the above comparison is by no means conclusive but it does seem reasonable to use the FRNL form of the

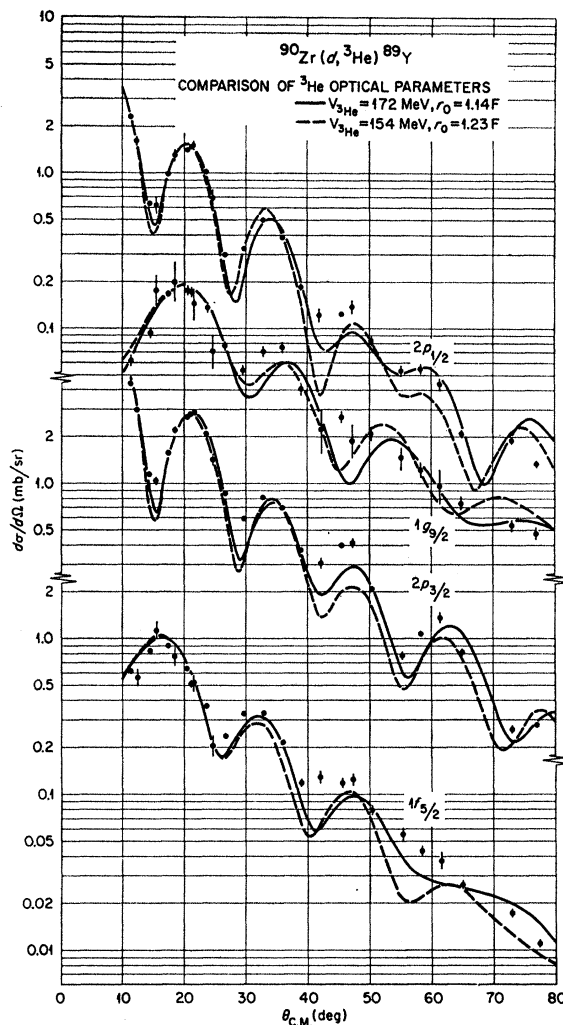


FIG. 5. Comparison of distorted-wave predictions for the two sets of ${}^3\text{He}$ optical parameters presented in Table II.

theory with the 172-MeV ${}^3\text{He}$ potential in the following analyses.

B. ${}^{92}\text{Zr}(d, {}^3\text{He}){}^{91}\text{Y}$

The observed differential cross sections for reactions leading to seven states in ${}^{91}\text{Y}$ are shown in Fig. 6. Except for distributions I and III, all of the curves are the FRNL calculations and have been normalized to the data by minimizing χ^2 over the entire angular region. The curves shown with the first and third excited groups, labeled $2p_{3/2}+1g_{9/2}$ and $2p_{3/2}+1f_{5/2}$, respectively, will be discussed below.

From the figure it is seen that the ground state is well fitted by a $2p_{1/2}$ proton transfer as was the case for the ${}^{90}\text{Zr}(d, {}^3\text{He}){}^{89}\text{Y}$ ground-state reaction. State II at 0.91 MeV is well described by a $1f_{5/2}$ pickup and the state at 2.21 MeV is best described also by a $1f_{5/2}$ pickup, although the apparent rise at forward angles is not accounted for. The states IV and VI are shown

²² S. M. Shafroth, P. N. Trehan, and D. M. Van Patter, Phys. Rev. **129**, 704 (1963); D. M. Van Patter and S. M. Shafroth, Nucl. Phys. **50**, 113 (1964); J. Alster, D. C. Shreve, and R. J. Peterson, Phys. Rev. **144**, 999 (1966).

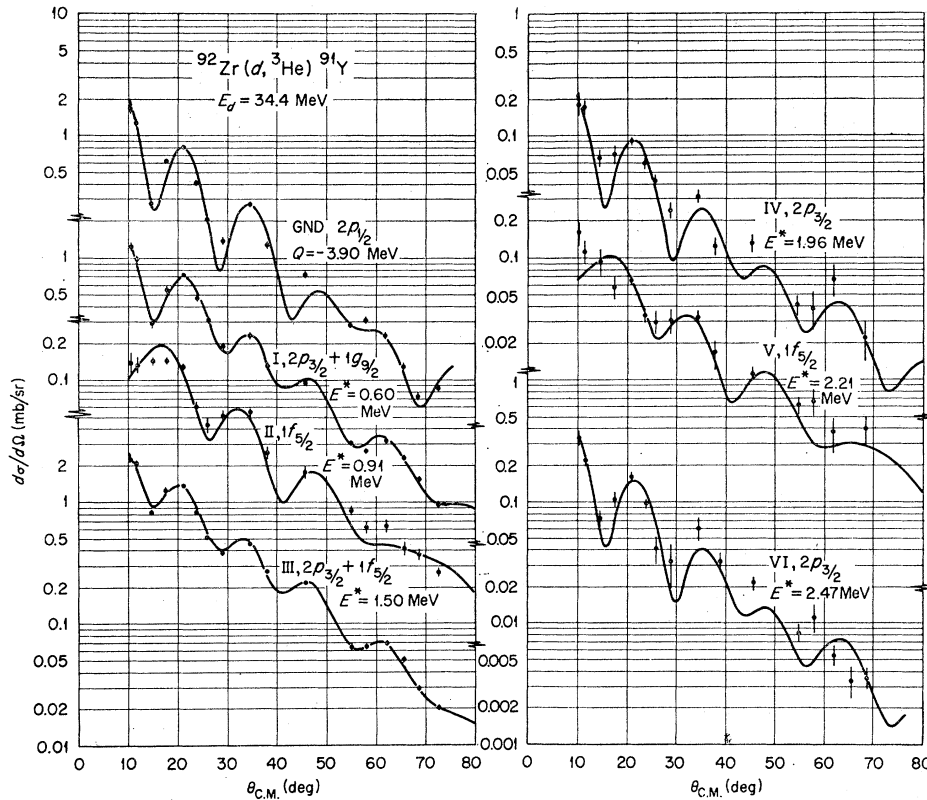


FIG. 6. Angular distributions for $^{92}\text{Zr}(d,^3\text{He})^{91}\text{Y}$. The curves for states I and III are discussed in the text. The other curves are FRNL distorted-wave calculations.

with the prediction for a $2p_{3/2}$ transfer, although the data lack the statistics to make this j assignment definite. Since the simple shell-model picture presented in Sec. III B predicts one $2p_{1/2}$ transfer and four $2p_{3/2}$ transfers, these states have been analyzed as $\frac{3}{2}^+$.

As was seen for ^{90}Zr , the DW theory predicts shapes for the angular distributions which are in good agreement with the data. However, these shapes do not provide exact fits. Therefore, to get the true shape for any of the observed proton transfers, one may take the experimental shapes from the measured distributions in the $^{90}\text{Zr}(d,^3\text{He})^{89}\text{Y}$ reaction since the states are well resolved and the relative errors are small. For smooth variations with mass and Q , this method then provides one with "exact" shapes in this mass and energy region that can be used in quantitative analyses of data. The use of such an approach in two cases will now be discussed.

The differential cross sections for groups I and III presented in Fig. 6 arise from apparent doublets at 0.60 and 1.50 MeV. It is known²³ that the $\frac{3}{2}^+$ isomeric state in ^{91}Y lies at 0.551 MeV and thus, in this reaction with 125-keV resolution (FWHM), it would be unresolved from the state at 0.645 MeV tentatively assigned $\frac{3}{2}^-$. Therefore, a $1g_{9/2}$ experimental shape has been summed with a $2p_{3/2}$ shape because of the obvious

$l=1$ character of the distribution, shown by the sharp rise at forward angles. The relative amounts of p and g strength were determined by requiring a minimum χ^2 fit to the data:

$$\chi^2 = \sum_i \left[\frac{A\sigma_p(i) + B\sigma_g(i) - \sigma_{\text{exp}}(i)}{\Delta\sigma_{\text{exp}}(i)} \right]^2.$$

The curve shown with the data is the result of this sum. The group at 1.50 MeV has been analyzed as an unresolved doublet arising from a $2p_{3/2}$ transfer and a $1f_{5/2}$ transfer. Again the curve shown with the data is the result of the sum which minimizes χ^2 using the experimental shapes from the $^{90}\text{Zr}(d,^3\text{He})^{89}\text{Y}$ reaction. This summation can be justified in the following manner. If this assumption is correct, then a sum of the data for the second ($2p_{3/2}$) and third ($1f_{5/2}$) excited states of ^{89}Y should have the same shape as the angular distribution of the group in question. This sum is shown as the second distribution in Fig. 7. The data for the reactions to the group at 1.50 MeV have been shown again in the first distribution for comparison. The sum of the ^{89}Y states has been normalized to the height of the ^{91}Y distribution. The curves shown with the distributions are identical to the curve shown with the data for the 1.50-MeV group in Fig. 6. Thus, by comparing the two, one can conclude that the data for the 1.50-MeV group in ^{91}Y most probably arises from an un-

²³ D. P. Ames, M. E. Bunker, L. M. Langer, and B. M. Sorenson, Phys. Rev. **91**, 68 (1953).

resolved $\frac{3}{2}^-$ and $\frac{5}{2}^-$ level. As a check, the same type of analysis was made assuming a $2p_{1/2}$ transfer rather than the $2p_{3/2}$ transfer. Although the j dependence is more subtle than that for the resolved proton transfers from ${}^{90}\text{Zr}$, the data show some preference for the $2p_{3/2}$ assignment. The spectrograph data resolve the doublets of groups I and III. On the basis of the above argument and the relative strengths of the $l=1$ and $l=3$ strengths deduced by fitting the 1.5-MeV group, it is possible to tentatively assign the lower 1.47-MeV member as $\frac{3}{2}^-$ and the upper state at 1.53 MeV as $\frac{5}{2}^-$. We would also confirm the $\frac{3}{2}^+$ assignment for the 0.645-MeV level. Evidence from the high-resolution spectrum indicates group VI is also a doublet and this is evident from its width in Fig. 1. However, the statistics are such that no reliable separation into components is possible.

In Fig. 4(b) the excitation energies, spins, and parities determined in this work are compared with those obtained by Ames *et al.*²³ from the β^- decay of ${}^{91}\text{Sr}$. The spin and parity assignments enclosed in parentheses are their proposed values. This experiment, which is sensitive to hole states, presents six new levels. Theoretical calculations by Ball²⁴ predict a low-lying $\frac{3}{2}^+$ state at 0.57 MeV and also predict a $\frac{3}{2}^-$ state at 0.73 MeV and a $\frac{5}{2}^-$ state at 0.90 MeV. Similar calculations have been reported by Vervier.² The $\frac{5}{2}^-$ predictions are in good agreement with the observed $\frac{5}{2}^-$ level at 0.91

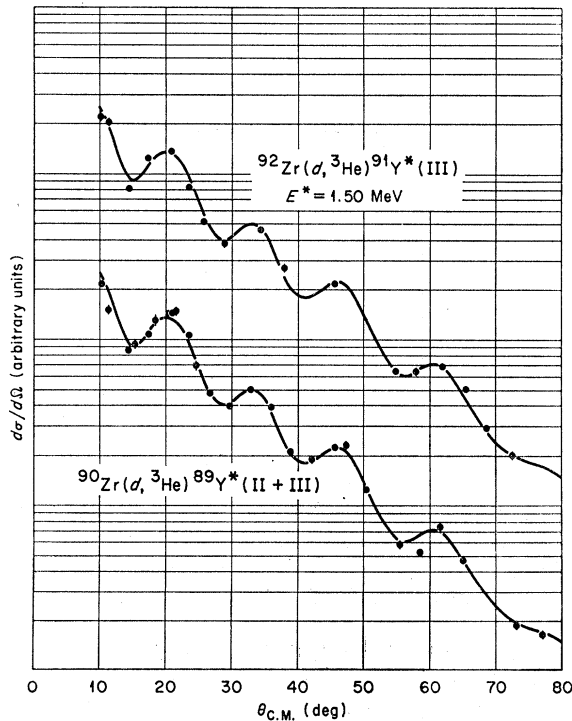


FIG. 7. Characteristic shape of a summed $2p_{3/2}+1f_{5/2}$ angular distribution.

²⁴ J. B. Ball (private communication).

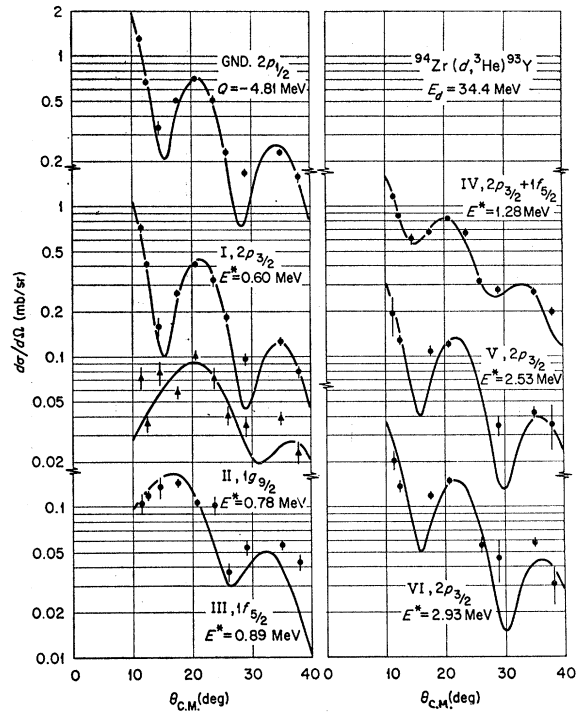


FIG. 8. Angular distributions for ${}^{94}\text{Zr}(d, {}^3\text{He}){}^{93}\text{Y}$. The curve for state IV is discussed in the text. The remaining curves are FRNL distorted-wave calculations.

MeV and the predicted $\frac{3}{2}^-$ level lies close to the published level at 0.645 MeV.

C. ${}^{94}\text{Zr}(d, {}^3\text{He}){}^{93}\text{Y}$

The angular distributions for $(d, {}^3\text{He})$ reactions leading to seven states or groups of states in ${}^{93}\text{Y}$ are presented in Fig. 8. The curves shown with the data are the FRNL calculations for all but group IV at 1.28 MeV. This distribution has the shape characteristic of the $p+f$ sum discussed in the preceding section and it has been analyzed as such. The curve shown with the data results from the summation of the appropriate ${}^{90}\text{Zr}(d, {}^3\text{He}){}^{89}\text{Y}$ experimental shapes. Since the data were only taken at laboratory angles of $\leq 37^\circ$, all $l=1$ proton transfers are ambiguous as to j value. However, the simple shell-model picture presented in Sec. III B predicts $\frac{1}{2}^-$ for the ground state and four $\frac{3}{2}^-$ excited states. The ground and three excited states at 0.599, 2.53, and 2.93 MeV all have $l=1$ shapes and have been assigned spins accordingly for the extraction of spectroscopic factors. The $l=1$ component of group IV completes the expected quartet of $\frac{3}{2}^-$ states. State III at 0.890 MeV shows the characteristics of an $l=3$ transfer and although the forward angle data for state II lacks continuity, it is best fit by an $l=4$ transfer and has been analyzed as a $\frac{3}{2}^+$ state.

Figure 4(c) presents a comparison of the energy levels observed in this work with those published by

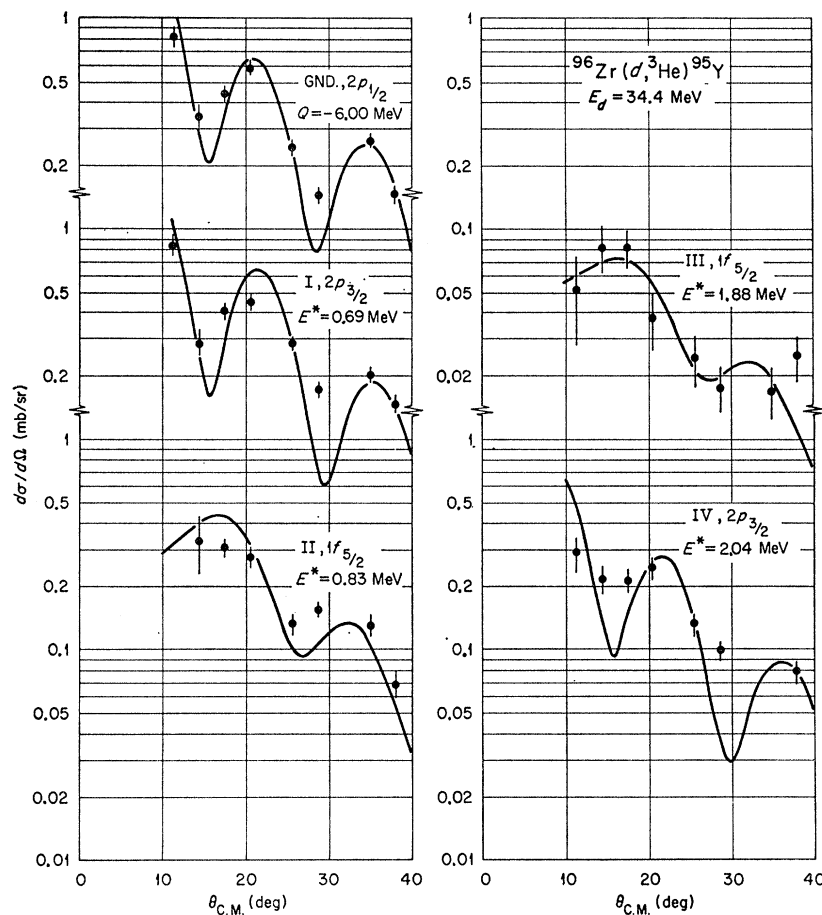


FIG. 9. Angular distributions for $^{96}\text{Zr}(d,^3\text{He})^{95}\text{Y}$ with FRNL distorted-wave calculations.

Prestwich *et al.*²⁵ and by Bakhru and Mukherjee.²⁶ There is obvious disagreement between the two level schemes, although both sets of levels were obtained from the β^- decay of ^{93}Sr and subsequent γ cascades in ^{93}Y . Prestwich *et al.* obtained ^{93}Sr as a fission fragment from the $^{235}\text{U}(n,f)$ reaction. Bakhru and Mukherjee produced ^{93}Sr from the $^{96}\text{Zr}(n,\alpha)^{93}\text{Sr}$ reaction. The present work agrees well with the energy-level scheme of Prestwich *et al.*

Another point should be made concerning the ^{93}Y levels. Neither of the above decay scheme studies observed an expected isomeric transition in the γ decay. The present work provides an explanation of this result if, as above, we make the reasonable assumption that the $l=1$ transition to the 0.60 MeV level excites a $\frac{3}{2}^-$ hole state. Thus this first $\frac{3}{2}^-$ level is found to lie below the $\frac{3}{2}^+$ level (0.78 MeV) and the $\frac{3}{2}^+$ state can decay to it by an $E3$ transition rather than by an isomeric $M4$ transition to the $\frac{1}{2}^-$ ground state. The fact that Prestwich *et al.* found their level at 0.775 MeV decayed only through the level at 0.597 MeV further supports this view.

²⁵ W. V. Prestwich, K. Fritze, and T. J. Kennett, Nucl. Phys. **37**, 45 (1962).

²⁶ H. Bakhru and S. K. Mukherjee, Nucl. Phys. **61**, 56 (1965).

D. $^{96}\text{Zr}(d,^3\text{He})^{95}\text{Y}$

The data and FRNL calculations for the ground and four excited states observed in the $^{96}\text{Zr}(d,^3\text{He})^{95}\text{Y}$ reaction are shown in Fig. 9. As for the $^{94}\text{Zr}(d,^3\text{He})^{93}\text{Y}$ states, data were not taken beyond a lab angle of 37° and thus it was not possible to test the j dependence for the $l=1$ transfers. However, within the framework of the simple shell model and for purposes of spectroscopic analysis, the ground state has been taken as $\frac{1}{2}^-$ and the two excited $l=1$ states at 0.69 and 2.04 MeV as $\frac{3}{2}^-$. A $\frac{1}{2}^-$ assignment for the ground state of ^{95}Y agrees with that of Larson and Gordon²⁷ but disagrees with the $\frac{5}{2}^-$ speculation by Van Klinken *et al.*²⁸ Since the ground-state transfer is unambiguously an $l=1$ pickup, an assignment of $\frac{1}{2}^-$ seems quite reasonable. The states at 0.83 and 1.88 MeV are the result of $l=3$ transfers.

The energy levels, with their spin and parity assignments, observed in this work are shown in Fig. 4(d). Previously, no levels were known in ^{95}Y . It should be noted that no $\frac{3}{2}^+$ state was observed in this reaction.

²⁷ R. E. Larson and C. M. Gordon, Nucl. Phys. **88**, 481 (1966).

²⁸ J. Van Klinken, L. M. Taff, G. W. Eakins, A. J. Bureau, and E. N. Hatch, Phys. Rev. **154**, 1116 (1967).

This is a point of some concern since, from the results of the preceding sections, one would expect a $\frac{3}{2}^+$ particle state to exist in ⁹⁵Y and that it should be reached by this reaction. However, with the large negative Q values involved in the ⁹⁶Zr($d, ^3\text{He}$) reaction and the relative fullness of the $(2p_{1/2})^2$ configuration to be discussed in the following section, one predicts the cross section for a $1g_{9/2}$ proton pickup to be quite weak (~ 0.03 mb/sr at the 20° peak). Thus the fact that no such state was seen is probably due to inadequate statistics and/or the possibility of inadequate resolution. Since no isomeric transition has been observed in ⁹⁵Y, this state probably lies at higher excitation than state I (0.69 MeV; $\frac{3}{2}^-, \frac{1}{2}^-$). From the known Q values of the isotopic impurities in the ⁹⁶Zr target, a new value of -81.225 ± 0.025 MeV for the mass excess of ⁹⁵Y has been experimentally determined. This value refines the estimate of -81.46 ± 1.0 MeV published by Mattauch *et al.*¹³

V. DISCUSSION

A. Spectroscopic Factors

The differential cross section for the ($d, ^3\text{He}$) reaction can be written in terms of the computed distorted-wave cross section $\sigma_{\text{DW}}(\theta)$ as

$$d\sigma/d\Omega = 2.95C^2S(l, j)\sigma_{\text{DW}}(\theta). \quad (1)$$

The normalization of 2.95 was estimated by Bassel from the overlap of model deuteron and ³He wave functions.¹⁵ He suggests that due to various uncertainties in the quantities used in the calculations, this value is uncertain to the order 30%.¹⁸ The quantity C is the isospin Clebsch-Gordan coefficient $\langle T_{B\frac{1}{2}}, M - mm | T_A M \rangle$ where $M = T_A = (N - Z)/2$ of the target and $m = -\frac{1}{2}$ for this reaction and $S(l, j)$ is the isospin spectroscopic factor. From the least-squares normalization of the FRNL calculations to the experimental angular distributions, the absolute spectroscopic factors (C^2S) are obtained by Eq. (1). The values of C^2S for each observed state are shown in Table III. These factors result from DW calculations using the bound-state parameters $r_0 = 1.20$ F, $r_c = 1.25$ F, $a = 0.65$ F, and $\lambda = 25$. The limits of C^2S predicted by the model presented in Sec. III B are presented at the bottom of the table. One could now place an uncertainty of about 35% on the numbers in this table by taking into account the 15% experimental uncertainty on the absolute cross sections and the 30% uncertainty of Bassel's normalization. However, due to the extreme sensitivity of σ_{DW} to the parameters r_0 and a in the assumed Woods-Saxon well, the agreement of the majority of the values of C^2S to within 30% of the model limits is encouraging. Until the bound-state parameters are determined to about 1%, the fluctuations presented in Table I will be a dominant factor in the accuracy of absolute spectroscopic factors.

Relative values of C^2S are free of the uncertainty of the deuteron-³He overlap, but are still subject to both experimental and theoretical uncertainties. The experimental errors arise from cross-section values for pickup to different states in each isotope and are taken at 5%. For the three states that were analyzed as doublets (⁹¹Y, $E^* = 0.60$ and 1.50 MeV; and ⁹³Y, $E^* = 1.28$ MeV) the relative cross sections have larger uncertainties of 10–15% due to the method of extraction. The theoretical uncertainties arise from the ability of the DW analysis to correctly predict the relative (n, l, j) and Q dependence. From Table I, it can be seen that the relative values of the calculations are not sensitive to the choice of r_0 , a , and λ . However, the uncertainties in the optical potentials, the form of the bound-state well, and various complexities in the calculations themselves would lead Bassel to estimate a relative error of 10–15%.¹⁸

The lack of consistency in the values $\sum[C^2S(2p_{1/2}) + C^2S(1g_{9/2})]$ and $\sum C^2S(2p_{3/2})$ between ⁹⁰Zr and the other isotopes is rather large to be solely accounted for by experimental uncertainties. The changes may be real, but it seems reasonable to attribute them to some inaccuracy in the DW calculation. For example, the fact that there are $2d_{5/2}$ neutrons for all of the isotopes except ⁹⁰Zr suggests that an adjustment to the bound-

TABLE III. Absolute values of C^2S from the ($d, ^3\text{He}$) reaction on the even isotopes of zirconium.^a

Residual nucleus	Excitation energy (MeV)	$1g_{9/2}$	$2p_{1/2}$	$2p_{3/2}$	$1f_{5/2}$
⁹⁰ Y	0.0		1.91		
	0.91	1.10			
	1.51			4.25	
	1.75				7.80
	$\sum C^2S$	1.10	1.91	4.25	7.80
⁹¹ Y	0.0		1.33		
	0.60	1.09		0.84	
	0.91				1.50
	1.50			1.90	5.28
	1.96			0.21	
	2.21				1.21
	2.47			0.38	
$\sum C^2S$	1.09	1.33	3.33	7.99	
⁹³ Y	0.0		1.58		
	0.60			0.89	
	0.78	0.81			
	0.89				1.70
	1.28			1.51	4.00
	2.53			0.51	
	2.93			0.66	
$\sum C^2S$	0.81	1.58	3.57	5.70	
⁹⁵ Y	0.0		2.08		
	0.69			1.90	
	0.83				6.24
	1.88				1.47
	2.04			1.41	
$\sum C^2S$...	2.08	3.31	7.71	

^a Model limits:

$$\sum C^2S(1g_{9/2}) + \sum C^2S(2p_{1/2}) = 2; \sum C^2S(2p_{3/2}) = 4; \sum C^2S(1f_{5/2}) = 6.$$

TABLE IV. Coefficients for $(2p_{1/2})^2$ and $(1g_{9/2})^2$ terms in the zirconium ground-state wave functions. See text for a discussion of uncertainties in A^2 and B^2 .

Isotope	Experiment		Theory ^a	
	A^2	B^2	A^2	B^2
⁹⁰ Zr	0.64	0.36	0.644	0.356
⁹² Zr	0.55	0.45	0.579	0.389
⁹⁴ Zr	0.66	0.34	0.634	0.351
⁹⁶ Zr	0.86	0.14	0.709	0.291

^a Reference 24.

state well may be required to account for this. It also seems plausible to assign $\frac{3}{2}^-$ to the excited $l=1$ transfers in ^{91,93,95}Y since any $\frac{1}{2}^-$ assignment would reduce further the total $2p_{3/2}$ spectroscopic strength. The low value of $C^2S(1f_{5/2})$ for ⁹⁴Zr can be attributed to some of the expected strength being in unobserved levels at higher excitation, particularly since the cross sections for this l transfer are low.

B. Nuclear Structure

The spectroscopic factors presented in the previous section may be interpreted in terms of the shell-model configurations in the zirconium ground state. In Sec. III B explicit forms for the zirconium wave functions were presented in terms of the two protons outside of these closed shells. Since the squares of the coefficients, A and B , represent the probability that the nucleus is in the configurations $(2p_{1/2})^2$ and $(1g_{9/2})^2$, respectively, the relative spectroscopic strengths for the observed $2p_{1/2}$ and $1g_{9/2}$ proton transfers provide a direct measurement of this admixture. These coefficients can be obtained from Table III. However, if one chooses to renormalize Table III in accordance with this simple model, the spectroscopic strength for the $2p_{3/2}$ transfers is consistently low. This could be interpreted as an indication that a $(2p_{3/2})^{-2}$ configuration exists in the zirconium ground states. However, since the lack of spectroscopic strength can be ascribed to experimental and/or theoretical analysis, the data presented here cannot prove conclusively that this apparent two-particle, two-hole contribution is real. Therefore, this possibility was not considered further. The $(^3\text{He},d)$ stripping reaction, which would be sensitive to such configurations, is now being used in a study involving these same zirconium isotopes.

The values obtained of A^2 and B^2 for each isotope are shown in Table IV. Errors of approximately 0.05 may be assigned to the values of A^2 for ⁹⁰Zr, ⁹²Zr, and ⁹⁴Zr from purely experimental considerations. In addition to these experimental uncertainties, as previously mentioned, are the 10–15% uncertainties in the DW

calculations for different l transfers. The coefficients for ⁹⁶Zr have larger experimental error (0.1) than those for the other isotopes. This is due to the fact that no $\frac{3}{2}^+$ state was seen in ⁹⁵Y. An estimate of this p - g admixture may be made by noting that the $C^2S(2p_{3/2})$ and $C^2S(1f_{5/2})$ are comparable for ⁹²Zr and ⁹⁶Zr. Thus by using the same renormalization for these two isotopes the difference between values of $C^2S(2p_{1/2})$ is taken as an indication of different populations in the $(2p_{1/2})^2$ configuration.

There is good agreement between the values of A^2 and B^2 for the ⁹⁰Zr ground-state mixture found in this work and previously determined values. The comparison for A^2 is experimentally: 0.64 ± 0.05 (this work), 0.70 ± 0.07 (Fulmer and Ball¹²), 0.55 ± 0.11 (Yntema⁶), 0.63 ± 0.05 (Bayman *et al.*⁹), 0.60 (Kavaloski *et al.*⁷); and theoretically: 0.644 (Ball²⁴), 0.64 (Cohen *et al.*¹⁰), and 0.62 (Vervier²). One exception is the value of 0.71 ± 0.03 obtained by Day *et al.*¹¹ from the $(^3\text{He},d)^{90}\text{Zr}$ reaction.

It should be pointed out that since only one $\frac{3}{2}^+$ level was observed in ⁹¹Y and ⁹³Y, the individual coefficients B' , B'' , and B''' for ⁹²Zr and ⁹⁴Zr would not be determined. However, since one expects the coefficients of the 2^+ and 4^+ couplings to be small, the error involved in presenting just A^2 and B^2 for ⁹²Zr and ⁹⁴Zr should be absorbed in the larger experimental uncertainty.

Also shown in Table IV are values calculated by Ball²⁴ for the other zirconium isotopes. In these calculations he used proton-neutron interaction matrix elements obtained from other experimental work in this region that were modified in a reasonable way in order to produce the agreement with this work. From this table, one can see that the $2d_{5/2}$ neutron shell does affect the proton configuration admixture in the ground states of the zirconium isotopes. The amount of $(2p_{1/2})^2$ strength decreases from 63.5% in ⁹⁰Zr to 55% in ⁹²Zr and then increases to 86% in ⁹⁶Zr. This effect is attributed to the $(p-d)$ and $(g-d)$ proton-neutron interaction. It is also seen that shell-model calculations, which use realistic proton-neutron matrix elements, can reproduce the trend of this change in the $(2p_{1/2})^2 - (1g_{9/2})^2$ admixture.

ACKNOWLEDGMENTS

The authors wish to thank R. M. Drisko, R. H. Bassel, and J. B. Ball for their many helpful comments and discussions. The authors are also indebted to J. K. Dickens for making available the LEA computer code and to M. R. Cates for his help in accumulating the data. We also wish to acknowledge the complete cooperation given us by the operating crew of the ORIC.

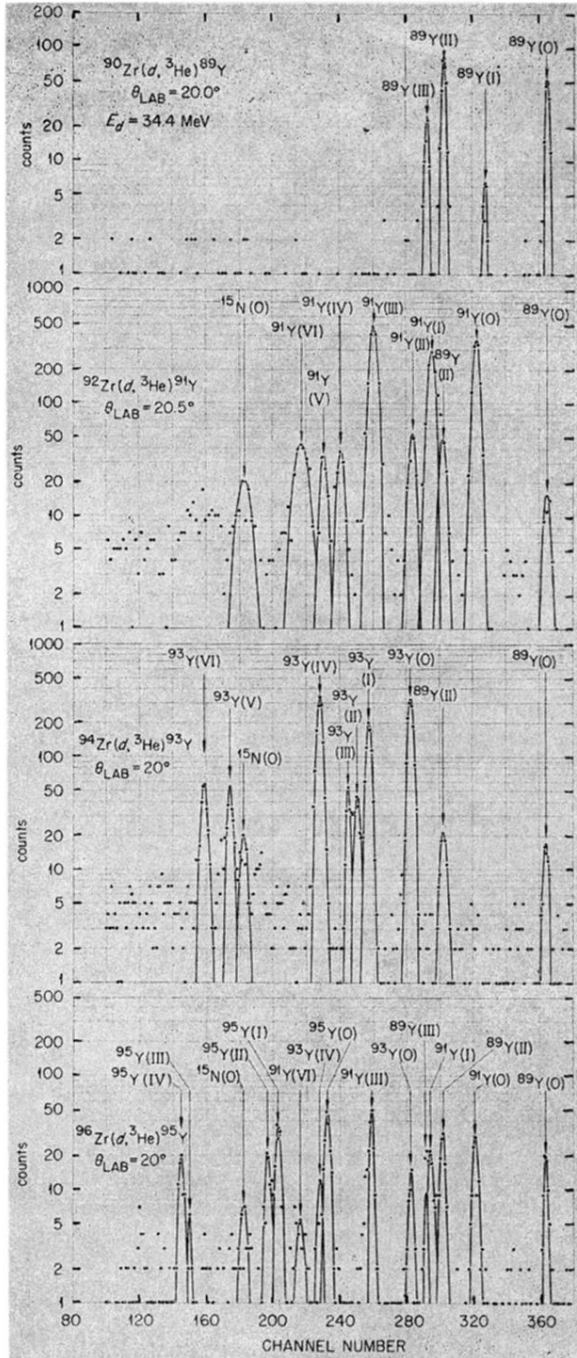


FIG. 1. Experimental spectra of ^3He particles resulting from $(d, ^3\text{He})$ reactions on ^{90}Zr , ^{92}Zr , ^{94}Zr , and ^{96}Zr .